PHOTONICS Research

Nonlinear interaction between broadband single-photon-level coherent states

Yuanhua Li,[1,2] Tong Xiang,[1,2] Yiyou Nie,[3] Minghuang Sang,[3] and Xianfeng Chen[1,2,*]

[1]State Key Laboratory of Advanced Optical Communication Systems and Networks, Department of Physics and Astronomy, Shanghai Jiao Tong University, Shanghai 200240, China
[2]Key Laboratory for Laser Plasma (Ministry of Education), Collaborative Innovation Center of IFSA (CICIFSA), Shanghai Jiao Tong University, Shanghai 200240, China
[3]Department of Physics, Jiangxi Normal University, Nanchang 330022, China
*Corresponding author: xfchen@sjtu.edu.cn

We experimentally demonstrate the nonlinear interaction between two chirped broadband single-photon-level coherent states. Each chirped coherent state is generated in independent fiber Bragg gratings. They are simultaneously coupled into a high-efficiency nonlinear waveguide, where they are converted into a narrowband single-photon state with a new frequency by the process of sum-frequency generation (SFG). A higher SFG efficiency of 1.06×10^{-7} is realized, and this efficiency may achieve heralding entanglement at a distance. This also made it possible to realize long-distance quantum communication, such as device-independent quantum key distribution, by directly using broadband single photons without filtering. © 2017 Chinese Laser Press

In quantum networks over optical fiber, narrowband single-photon-level coherent states at 1550 nm are well suited for numerous quantum communication tasks such as device-independent quantum key distribution (DI-QKD) [1–3] and quantum teleportation [4], as they can be easily produced with optical attenuators and can travel long distances with low loss transmission. It is well known that the true single photons at 1550 nm, which are produced in spontaneous parametric downconversion (SPDC) sources, are paramount in the development of future long-distance quantum communication. Unfortunately, these generated true single photons are broadband, and they are not suitable for long-distance quantum communication. Therefore, it is a problem to be solved in regards to how to use these broadband single photons directly in a future quantum network. However, the nonlinear interaction of single photons is not considered under most circumstances, as it is thought to be too weak to be observed. Realizing such an interaction is not only a fascinating challenge but also holds great applications for future quantum technologies.

It recently has been shown that nonlinear optics at the single-photon level can be more efficiently used to fulfill important quantum information processing tasks than the use of linear optics methods [5]. For example, a faithful entanglement swapping was realized without postselection by the process of sum-frequency generation (SFG). When the SFG

efficiency is larger than 10^{-8}, and assuming an overall detection and coupling efficiency of 60%, one heralded entangled-photon pair with fidelity $F \geq 0.9$ can be obtained. However, such SFG efficiency of 10^{-8} is extremely challenging to realize in common nonlinear organic materials or general nonlinear crystals [6–9]. Similar experimental results have been obtained [10,11], including the SFG from a narrowband single-photon-level coherent state and a narrowband single photon [10] and between two true narrowband single photons [11]. Nonlinear optical effects with the single photons have been experimentally demonstrated [12–15] but have significant implementation challenges that may hinder their uptake in conventional quantum communication tasks, as they impose restrictions on the wavelengths and bandwidths of single photons.

It has been demonstrated that parametric interactions hold numerous advanced applications in quantum information processing, but strong optical fields are usually used to preserve coherence [16]. Parametric interactions with a single photon pump have been experimentally observed, such as spontaneous downconversion [17] and cross-phase modulation [18]. Here we take the next step and report, for the first time to the best of our knowledge, a nonlinear interaction between two broadband single-photon-level coherent states. Note that our experiment cannot be seen simply as the repetitive process of the nonlinear interaction presented in Ref. [5]. Here we use

chirped technology to demonstrate the SFG between a positively chirped broadband single-photon-level coherent state and a negatively chirped broadband single-photon-level coherent state. The photons in all spectrums of the positively and negatively chirped coherent states are used to produce a narrowband single photon. Thus, our approach can improve the overall conversion efficiency of SFG. This has made it possible to realize long-distance quantum communication by using the true broadband single photons.

In our experiment, we increase the nonlinear interaction cross-section by strongly confining the input single photons, both spatially and temporally, over a long interaction length. The spatial confinement is obtained with a state-of-the-art periodically poled lithium niobate waveguide (PPLN-WG) chip, whereas the temporal confinement is achieved by using femtosecond pulsed light. The SFG efficiency is proportional to the square of the nonlinear WG length and inversely proportional to the duration of the input single photons. The nonlinear WG length is limited by the group velocity dispersion between the input photons and the unconverted photons [5]. The maximum SFG efficiency is guaranteed by matching the spectrotemporal characteristics of the photons with the quasi-phase-matching constraints of the PPLN-WG chip. A 5.2 cm PPLN-WG chip and 500 fs photons satisfy these conditions. In our work, the SFG efficiency of 1.06×10^{-7} is realized. Our approach highlights the potential for photon–photon interaction with an integrated device at room temperature and broadband single-photon-level coherent states at the 1550 nm telecom band, which will open the way toward novel applications in long-distance quantum communication tasks including DI-QKD.

A schematic of the experimental setup is shown in Fig. 1. Using a 50∶50 polarization maintaining beam splitter (BS), the mode-locked optical fiber laser can generate two copies of the pulses with equal energy. The two copies of the pulses are used to generate two broadband single-photon-level coherent states
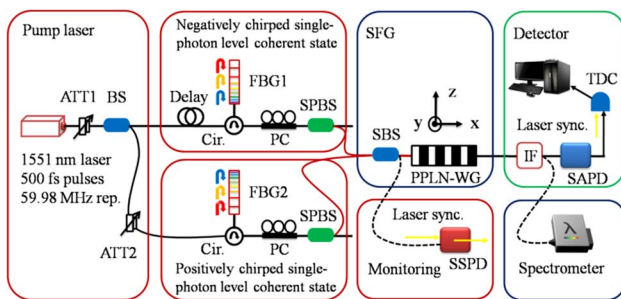
using two variable optical attenuators (ATT1 and ATT2) for this experiment. One of the two copies of the pulses is sent to a broadband fiber Bragg grating 1 (FBG1), and the other pulse is coupled into the FBG2. Both FBG1 and FBG2 possess the exact same parameters, such as the center wavelength of 1547 nm, FWHM bandwidth of 39 nm, and chirp rate of 5 nm/cm. Thus, the spectrums of two copies of the photons after FBG1 and FBG2 are the same but with the opposite sign. In our experiment, positively chirped single-photon level coherent states are generated through a broadband FBG2 to introduce a linear chirp by group velocity dispersion, and the other photons are negatively chirped photons from the other broadband FBG1.

As is known, an FBG can be used for up-chirping and down-chirping, depending on the choice of the side from which the light source is reflected. As the two copies of the pulses are from the same pump laser, they have the same initial center frequency ω_0. When two copies of the pulses with instantaneous frequencies, described as $\omega_1(t) = \omega_0 + At$ and $\omega_2(t) = \omega_0 - At$ (where A is the linear chirp parameter) undergo sum-frequency mixing, the instantaneous frequency of the generated pulse is constant $[\omega_1(t) + \omega_2(t) = 2\omega_0]$; thus, the long narrowband pulse is realized [19].

Subsequently, the positively and negatively chirped coherent states are coupled into the z-cut PPLN-WG chip by the fiber pigtail. The PPLN-WG chip is a 5.2 cm long reverse-proton-exchange WG that is quasi-phase matched to carry out the SFG process 1551 nm + 1551 nm → 775.5 nm. The WG has a quasi-phase-matching (QPM) period of 19.6 μm, which incorporated single-mode filters designed to match the single-mode size of SMF-28 optical fiber. Two 200∶1 single-mode polarization beam splitters (SPBS) and two polarization controllers (PCs) are used for controlling the positively and negatively chirped coherent states to the TM mode. A superconducting single photon detector (SSPD) is used to calibrate and monitor the counts of the positively and negatively chirped photons, whose detection efficiency is up to 10% at 1551 nm, and the dark count rate is 600 Hz. A stable temperature controller (TC) is used to keep the PPLN-WG chip's temperature at 27°C to maintain the QPM condition of the SFG process. The long narrowed single photons of higher frequency are generated after the interference filter (IF), with 20 nm FWHM bandwidth and 780 nm center wavelength (about 1.2 dB loss). Finally, the SFG photons are detected with a single-photon detector, whose detection efficiency is up to 60% at 775 nm, and the dark count rate is about 26 Hz. The SFG photons and the laser clock signal are recorded using a time-to-digital converter.

We first measure the spectrums of the negatively chirped light (called pump light) and the positively chirped light (called signal light) by using an optical-fiber-coupled spectrometer, which are shown in Fig. 2(a). The pump light (800 ± 20 GHz spectral FWHM bandwidth, and 1551.56 nm center wavelength) is then coupled into the PPLN-WG chip with the signal light (790 ± 20 GHz FWHM, and 1551.56 nm center wavelength) using SFG. The created upconverted light, after IF, is sent into the spectrometer.

In our experiment, when the classical pump and signal laser pulses are sent to the PPLV-WG chip, the upconverted photons
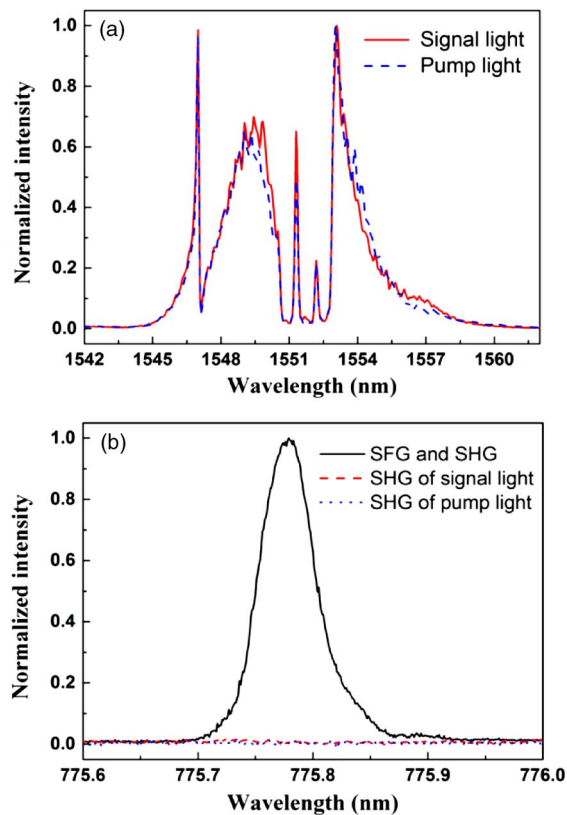

Fig. 1. Experimental setup. A mode-locked optical fiber laser generates 500 fs pulses at 1551 nm with a repetition of 59.98 MHz and is used to generate the two chirped broadband single-photon-level coherent states based on FBG1 and FBG2. The two chirped broadband coherent states are combined via a 50∶50 single-mode beam splitter (SBS) and directed to a 5.2 cm long fiber pigtailed Type-0 PPLN-WG chip. The total losses in the WG are 2.2 dB, such as a coupling loss of about 0.7 dB and a total fiber-to-output-facet loss of approximately 1.5 dB. The unconverted photons are deterministically separated from the SFG photons by an IF, and the SFG photons are sent to a single photon detector (silicon APD). The entire experiment is fiber-coupled.

Fig. 2. (a) Pump and signal light spectrums. (b) Spectrums of upconverted light (SFG and SHG): SHG of signal light; SHG of pump light.

consist of second-harmonic generation (SHG) of pump photons, SHG of signal photons, and SFG of pump photons and signal photons. Although upconverted single photons cannot be separately distinguished, the SFG photons N_{SFG} can be measured. First, the pump photons are coupled into the WG alone, the SHG photons N_1 are detected. Similarly, the SHG photons N_2 of signal photons are obtained when only the signal photons are subjected to the WG alone. When we simultaneously send the two independent photons together to the WG, we can measure the photons N_0 of SFG and SHG. Therefore, the SFG photons are calculated according to the equation $N_{SFG} = N_0 - N_1 - N_2$. For the SFG photons to be measured distinctly, any residue of pump and signal light has to be filtered out from upconversion photons by a factor of 10^{-18} in this work. Here, the SFG efficiency is given by $\eta_{SFG} = N_{SFG}/N_A$, where N_A is the number of photons per second of the signal light.

For instance, we control the input energy of the signal and pump light, which is 200.2 and 200.4 μJ, respectively. When they are simultaneously coupled into the PPLN-WG chip, the FWHM bandwidth and energy of the created photons can be measured. If pump light (or signal light) is sent to the PPLN-WG chip alone, the bandwidth and energy of SHG can be obtained. When the PPLN-WG chip's temperature is kept at 27°C, as shown in Fig. 2(b), the FWHM bandwidth of the created photons is about 0.07 nm, centered at 775.78 nm. In this case, the energy of produced harmonics is 20.9 μJ

(involving the SFG and SHG), which is obtained from SHG of signal light (0.25 μJ), SHG of pump light (0.01 μJ), and SFG (20.54 μJ). The maximum SFG efficiency of 5% is realized, which is used to estimate the SFG efficiency in our proposal. As shown in Fig. 3, the SFG efficiency depends on the PPLN-WG chip's temperature. Correcting for all of these losses, the intrinsic device maximum SFG efficiency of 20% is obtained, as expected.

When the number of photons per pulse of pump photons and signal photons is attenuated to 5.13 and 5.64, respectively, the detected SHG count of signal photons (or pump photons) drops to its dark count (about 3.8 Hz). It can be verified that any photon detected by the SPAD is the result of the SFG process when the signal and pump power are simultaneously attenuated to single-photon-per-pulse. Therefore, their own SHG photons are not considered in these situations.

In our experiment, the number of photons per pulse (equal for pump and signal) are obtained by attenuating ATT1 and ATT2, as they can be detected and calibrated by the SSPD. According to our experimental data, the SFG efficiency and SFG photons are shown in Fig. 4.

It has been demonstrated that the SFG photons are proportional to the square of the pump photons per pulse, which is in complete agreement with our experimental result. It is known that the SFG efficiency is proportional to the square of the PPLN-WG chip length L^2 and inversely proportional to the pump power E. If the pump power is reduced to one-photon-per-pulse, the power of pump is calculated as the energy of each photon divided by its coherence time, which is described as $E = hc\Delta\nu/(\lambda tbp)$ [5]. Here, λ denotes the center wavelength of pump photons, tbp is the time-bandwidth product, and $\Delta\nu$ represents the pump photon bandwidth. Furthermore, the pump photon bandwidth decreases linearly with the length of the PPLN-WG chip and is given by $\Delta\nu = \Delta\hat{\nu}/L$, where $\Delta\hat{\nu} \geq 4200 \text{ GHz} \cdot \text{cm}$ is the spectral acceptance of the PPLN-WG chip. Thus, the overall conversion efficiency of SFG is given by $\eta'_{SFG} = \xi(\lambda)hc\Delta\hat{\nu}L/(\lambda tbp)$, where $\xi(\lambda)$ denotes the measured upconversion efficiency of the PPLN-WG chip. Here, we experimentally demonstrate that such an equation holds by injecting a pair of one-photon-per-pulse beams at 1551.56 and
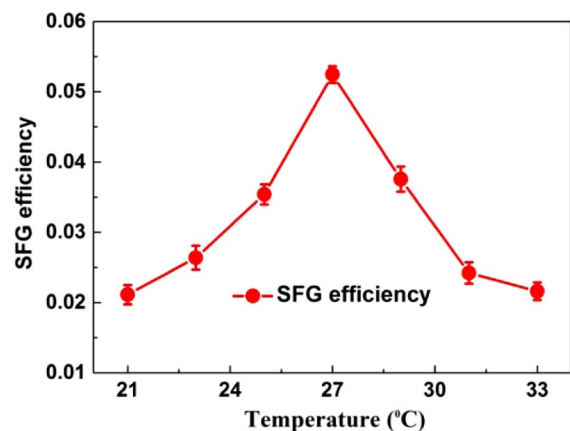

Fig. 3. SFG efficiency. SFG efficiency can be tuned by manipulating the PPLN-WG chip's temperature.
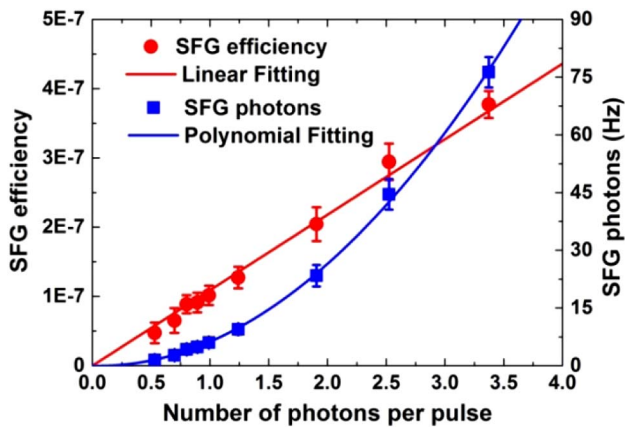
Fig. 4. SFG efficiency and SFG photons that the pump photons are upconverted when interacting with the signal photons inside the PPLN-WG chip, plotted against the number of photons per pulse (equal for signal and pump). Dark counts of 3.8 Hz have been subtracted, and the total losses of about 5.6 dB have been taken into account.

1551.56 nm into a 5.2 cm PPLN-WG chip and detecting the rate of 775.78 nm output photons [see Fig. 4].

Consider that $\xi(\lambda) = 5\%/(\mathrm{W} \cdot \mathrm{cm}^2)$ and $tbp = 0.4$ in our experiment; thus, the expected SFG efficiency is $\eta'_{\mathrm{SFG}} \approx 1 \times 10^{-7}$. We measure an efficiency of $\eta_{\mathrm{SFG}} = (1.06 \pm 0.23) \times 10^{-7}$, the SFG efficiency is high enough to provide efficient yet simpler solutions to linear-optics-based protocols for the heralded creation of maximally entangled pairs or for the implementation of DI-QKD. Note that our SFG efficiency is about eight times of the SFG efficiency obtained in Refs. [5,10,11]. When the single-photon-level pump and signal photons are not chirped in our experiment, the SFG photons are zero. This is because the intensity of pump light (or signal light) at 1551.56 nm is very low [see Fig. 2(a)]. However, when the negatively and positively chirped pulses are simultaneously sent together to the PPLN-WG chip, photons in all spectrums of the negatively and positively chirped light are used to produce the SFG photons. Therefore, we can improve the SFG efficiency by using the chirped technology.

Furthermore, if one uses the research device presented in Ref. [20] [10 cm nonlinear WG, $\xi = 100\%/(\mathrm{W} \cdot \mathrm{cm}^2)$], the SFG efficiency will increase to $\eta'_{\mathrm{SFG}} > 6 \times 10^{-7}$. When this 10 cm long nonlinear WG is used for the implementation of DI-QKD, one will achieve a rate of about 7 bits/min on a distance of 10 km. In the future, the SFG efficiency of nonlinear interactions between single photons will be further increased by exploiting highly nonlinear organic materials [21] or from the use of tighter field confinement [22].

In conclusion, we have experimentally demonstrated the SFG between two broadband single-photon-level coherent states by using a high-efficiency PPLN-WG chip. An integrated device at room temperature and broadband single-photon-level coherent states at telecom wavelengths are used in our experiment. Such single-photon-level nonlinear interactions will open exciting perspectives for future quantum technologies. At the level of SFG efficiency (1.06×10^{-7}) measured here, the result is already competitive with methods based on linear optics [23] and offers new possibilities such as heralding entanglement at a distance. This technique in our proposal marks a critical step toward the implementation of DI-QKD [24]. Furthermore, we believe that our demonstration of two broadband single-photon level coherent states will strongly stimulate research in nonlinear optics in the quantum regime. In addition, our approach has made it possible to realize long-distance quantum communication by using directly the true broadband single photons without filtering.

REFERENCES

1. N. Gisin, S. Pironio, and N. Sangouard, "Proposal for implementing device-independent quantum key distribution based on a heralded qubit amplifier," Phys. Rev. Lett. **105**, 070501 (2010).
2. Y. L. Tang, H. L. Yin, S. J. Chen, Y. Liu, W. J. Zhang, X. Jiang, L. Zhang, J. Wang, L. X. You, J. Y. Guan, D. X. Yang, Z. Wang, H. Liang, Z. Zhang, N. Zhou, X. F. Ma, T. Y. Chen, Q. Zhang, and J. W. Pan, "Measurement-device-independent quantum key distribution over 200 km," Phys. Rev. Lett. **113**, 190501 (2014).
3. M. Curty, F. H. Xu, W. Cui, C. C. W. Lim, K. Tamaki, and H. K. Lo, "Finite-key analysis for measurement-device-independent quantum key distribution," Nat. Commun. **5**, 3732 (2014).
4. Q. C. Sun, Y. L. Mao, S. J. Chen, W. Zhang, Y. F. Jiang, Y. B. Zhang, W. J. Zhang, S. Miki, T. Yamashita, H. Terai, X. Jiang, T. Y. Chen, L. X. You, X. F. Chen, Z. Wang, J. Y. Fan, Q. Zhang, and J. W. Pan, "Quantum teleportation with independent sources and prior entanglement distribution over a network," Nat. Photonics **10**, 671–675 (2016).
5. N. Sangouard, B. Sanguinetti, N. Curtz, N. Gisin, R. Thew, and H. Zbinden, "Faithful entanglement swapping based on sum-frequency generation," Phys. Rev. Lett. **106**, 120403 (2011).
6. G. Z. Li, Y. P. Chen, H. W. Jiang, and X. F. Chen, "Enhanced Kerr electro-optic nonlinearity and its application in controlling second-harmonic generation," Photon. Res. **3**, 168–172 (2015).
7. N. An, Y. L. Zheng, H. J. Ren, X. H. Zhao, X. W. Deng, and X. F. Chen, "Normal, degenerated, and anomalous-dispersion-like Cerenkov sum-frequency generation in one nonlinear medium," Photon. Res. **3**, 106–109 (2015).
8. X. L. Feng, Z. H. Wu, X. Y. Wang, S. L. He, and S. M. Gao, "All-optical two-channel polarization-multiplexing format conversion from QPSK to BPSK signals in a silicon waveguide," Photon. Res. **4**, 245–248 (2016).
9. J. F. Xia, S. Serna, W. W. Zhang, L. Vivien, and É. Cassan, "Hybrid silicon slotted photonic crystal waveguides: how does third order nonlinear performance scale with slow light?" Photon. Res. **4**, 257–261 (2016).
10. T. Guerreiro, E. Pomarico, B. Sanguinetti, N. Sangouard, J. S. Pelc, C. Langrock, M. M. Fejer, H. Zbinden, R. T. Thew, and N. Gisin, "Interaction of independent single photons based on integrated nonlinear optics," Nat. Commun. **4**, 2324 (2013).
11. T. Guerreiro, A. Martin, B. Sanguinetti, J. S. Pelc, C. Langrock, M. M. Fejer, N. Gisin, H. Zbinden, N. Sangouard, and R. T. Thew, "Nonlinear interaction between single photons," Phys. Rev. Lett. **113**, 173601 (2014).
12. T. Peyronel, O. Firstenberg, Q. Y. Liang, S. Hofferberth, A. V. Gorshkov, T. Pohl, M. D. Lukin, and V. Vuletić, "Quantum nonlinear optics with single photons enabled by strongly interacting atoms," Nature **488**, 57–60 (2012).
13. J. D. Pritchard, D. Maxwell, A. Gauguet, K. J. Weatherill, M. P. A. Jones, and C. S. Adams, "Cooperative atom-light interaction in a blockaded Rydberg ensemble," Phys. Rev. Lett. **105**, 193603 (2010).

14. K. M. Birnbaum, A. Boca, R. Miller, A. D. Boozer, T. E. Northup, and H. J. Kimble, "Photon blockade in an optical cavity with one trapped atom," Nature **436**, 87–90 (2005).

15. B. Dayan, A. Pe'er, A. A. Friesem, and Y. Silberberg, "Nonlinear interactions with an ultrahigh flux of broadband entangled photons," Phys. Rev. Lett. **94**, 043602 (2005).

16. R. T. Thew, H. Zbinden, and N. Gisin, "Tunable upconversion photon detector," Appl. Phys. Lett. **93**, 071104 (2008).

17. L. K. Shalm, D. R. Hamel, Z. Yan, C. Simon, K. J. Resch, and T. Jennewein, "Three-photon energy-time entanglement," Nat. Phys. **9**, 19–22 (2013).

18. N. Matsuda, R. Shimizu, Y. Mitsumori, H. Kosaka, and K. Edamatsu, "Observation of optical-fibre Kerr nonlinearity at the single-photon level," Nat. Photonics **3**, 95–98 (2009).

19. J. Lavoie, J. M. Donohue, L. G. Wright, A. Fedrizzi, and K. J. Resch, "Spectral compression of single photons," Nat. Photonics **7**, 363–366 (2013).

20. K. R. Parameswaran, R. K. Route, J. R. Kurz, R. V. Roussev, M. M. Fejer, and M. Fujimura, "Highly efficient second-harmonic generation in buried waveguides formed by annealed and reverse proton exchange in periodically poled lithium niobate," Opt. Lett. **27**, 179–181 (2002).

21. S. Kurimura, Y. Kato, M. Maruyama, Y. Usui, and H. Nakajima, "Quasi-phase-matched adhered ridge waveguide in LiNbO₃," Appl. Phys. Lett. **89**, 191123 (2006).

22. M. Jazbinsek, L. Mutter, and P. Gunter, "Photonic applications with the organic nonlinear optical crystal DAST," IEEE J. Sel. Top. Quantum Electron. **14**, 1298–1311 (2008).

23. C. Sliwa and K. Banaszek, "Conditional preparation of maximal polarization entanglement," Phys. Rev. A **67**, 030101 (2003).

24. J. Mower, Z. Zhang, P. Desjardins, C. Lee, J. H. Shapiro, and D. Englund, "High-dimensional quantum key distribution using dispersive optics," Phys. Rev. A **87**, 62322 (2013).